ACS EARTH AND SPACE CHEMISTRY

http://pubs.acs.org/journal/aesccq

Article

Impact of Hydrogen Sulfide on Photochemical Haze Formation in Methane/Nitrogen Atmospheres

Nathan W. Reed, Eleanor C. Browne,* and Margaret A. Tolbert

Cite This: *ACS Earth Space Chem.* 2020, 4, 897−904

Read Online

ACCESS | Metrics & More | Article Recommendations

ABSTRACT: The chemistry of trace sulfur gases in planetary organic haze formation is poorly understood, though both are ubiquitous in planetary atmospheres. Here, we perform laboratory studies to explore how the addition of trace amounts of H_2S (0.5−5 ppmv) affects organic aerosol produced from ultraviolet photochemistry of CH_4 in N_2. We analyze the aerosol product composition and size in real time. Inclusion of trace amounts of H_2S in the precursor mixture significantly enhances the formation of organic aerosol mass and the particle effective density, both of which increase as a function of initial H_2S concentration and in the absence of an additional carbon source. We further present evidence that the addition of trace H_2S to the precursor mixtures leads to the formation of organosulfur compounds. Their inclusion in the aerosol-phase contributes to the organic aerosol mass enhancement. Thiyl-alkene chemistry is proposed as a possible organosulfur formation mechanism. In contrast to previous assumptions that sulfur and carbon chemistry occur largely independently of each other, these results suggest a coupling between the two chemistries. This coupling has potential impacts on organic haze and atmospheric sulfur chemistry in planetary atmospheres.

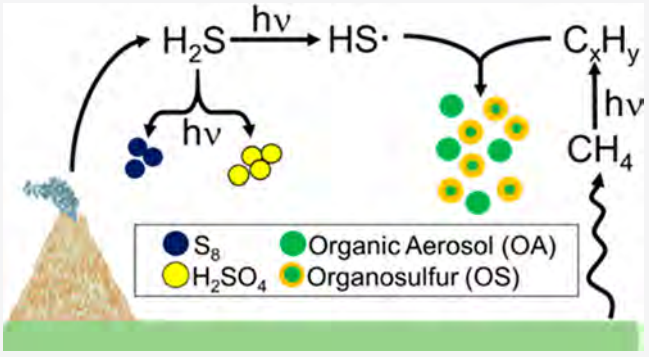

KEYWORDS: *organic haze, hydrogen sulfide, sulfur, organosulfur, Archean Earth, aerosol mass spectrometry*

INTRODUCTION

Sulfur gases, such as SO_2 and H_2S, are common in planetary atmospheres, and it is likely that they are ubiquitous constituents of exoplanetary atmospheres.[1−3] In our solar system, these gases are found in the atmospheres of Earth, Venus, Jupiter, and Jupiter's moon Io.[1,4,5] Sulfur gases are also of particular relevance for our understanding of the Archean Earth (4.0−2.5 billion years ago) as the mass-independent fractionation of sulfur isotopes (S-MIF) in Archean sediment records is currently the strongest evidence for an anoxic early atmosphere.[6] For S-MIF fractionation to occur, sulfur must leave the atmosphere in at least two chemically distinct reservoirs, currently thought to be as S_8 and H_2SO_4 aerosols.[7,8]

In Earth's current atmosphere, we know that a third sulfur reservoir exists—organosulfur. Moreover, the amount of organosulfur in the atmosphere is significant: organosulfates are estimated to comprise 5−10% of the modern-day organic aerosol mass.[9] Geochemical evidence suggests that organic aerosol also formed during the Archean via methane photochemistry, constituting what is known as organic haze.[10−12] Despite its known presence on modern Earth, current thought rarely considers organosulfur in the organic haze chemistry of the Archean or exoplanetary atmospheres. Most models of planetary atmospheres treat the chemistry of inorganic aerosol formation from H_2S and SO_2 largely independently from the methane photochemistry leading to organic aerosol formation.[2,13] The connection between organic compounds and sulfur compounds has typically been limited to indirect interactions. For example, by blocking relevant wavelengths of ultraviolet (UV) light, a periodic presence of organic haze aerosol in the Archean atmosphere could have altered SO_2 photolysis and consequently the S-MIF.[10−12,14] This is thought to be the primary cause of correlations in carbon and sulfur isotopes in Archean sediment records, observed as variations in the S-MIF magnitude before its permanent loss due to the rise of oxygen. In another example, Arney et al. (2018)[15] presents an organic haze model that includes organosulfur gases (such as CH_3SH and CH_3SCH_3), but only as additional hydrocarbon sources and excludes direct sulfur−carbon chemistry originating from H_2S or SO_2 (i.e., inorganic S).[15]

Received: April 6, 2020
Revised: May 8, 2020
Accepted: May 11, 2020
Published: May 11, 2020

https://dx.doi.org/10.1021/acsearthspacechem.0c00086
ACS Earth Space Chem. 2020, 4, 897−904

Although the chemistry of organic haze formation has been explored in laboratory experiments and atmospheric models, experimental investigation of the effects of atmospheric sulfur gases on organic haze is lacking. To the best of our knowledge, DeWitt et al.[16] presents the only laboratory study on the effects of a sulfur gas in photochemical methane haze formation.[16] They investigated how the addition of SO_2 perturbed methane haze photochemistry. Using aerosol mass spectrometry (AMS), DeWitt et al.[16] were able to identify specific organosulfur ions such as $CH_3SO_2^+$, CH_3SO^+, and CH_3S^+. These ions were attributed to organosulfates such as methyl sulfonic acid (MSA, CH_3SO_3H). Thus, these findings are in-line with organosulfur observations of modern Earth aerosol.

Laboratory studies on methane haze formation in the presence of another major atmospheric sulfur gas, H_2S, are completely absent from the literature. Although SO_2 is usually assumed to be the dominate volcanic sulfur gas emitted in planetary atmospheres, the relative amounts of H_2S and SO_2 in volcanic emissions vary and in some cases H_2S fluxes can dominate.[17,18] Atmospheric chemistry models have also shown that H_2S can accumulate in reducing atmospheres with low levels of oxygen,[19] conditions that are also favorable for organic haze formation.[20,21] Because H_2S gas is known to be produced by microbial sulfate reduction, the relevance of H_2S as a biosignature has also been debated.[2] In addition, microbial sulfate reduction is the oldest known form of metabolism and was likely prominent on the Archean Earth.[22]

To improve our understanding of organic haze and sulfur chemistry in reducing atmospheres, we conducted laboratory experiments to explore how the addition of trace amounts of H_2S to CH_4/N_2 mixtures affects photochemical methane haze formation. The composition, amount, and size of the aerosol products were monitored in real-time using a quadrupole aerosol mass spectrometer (Q-AMS) and a scanning mobility particle sizer (SMPS).

MATERIALS AND METHODS

Haze Aerosol Generation. The flow-through haze generation system (Figure 1) has been previously described in detail.[23−25] Briefly, gas mixtures with mixing ratios of 0.1% CH_4 (Airgas, 99.99%) and 0−5 ppmv H_2S (Airgas, 1000 ppmv H_2S in N_2) were mixed in a stainless-steel mixing cell in a nitrogen (N_2) background gas (Airgas, ultrahigh purity 99.998%) for at least 8 h in advance of each experiment. This CH_4 mixing ratio is within the range of values expected for the Archean Earth and reduced planetary atmospheres exhibiting a photochemical organic haze.[15,26] The H_2S mixing ratios were chosen to provide sulfur-to-methane ratios consistent with the sulfur-to-methane emission flux ratios of past modeling studies.[10−12,27] These ratios are broadly applicable to reduced atmospheres with either high volcanic activity or biological sulfate reduction, such as the Archean Earth or possibly rocky exoplanets.[2,18,28,29] Using fluxes as a metric for precursor mixing ratios is appropriate as our mixtures represent composition prior to photochemistry.

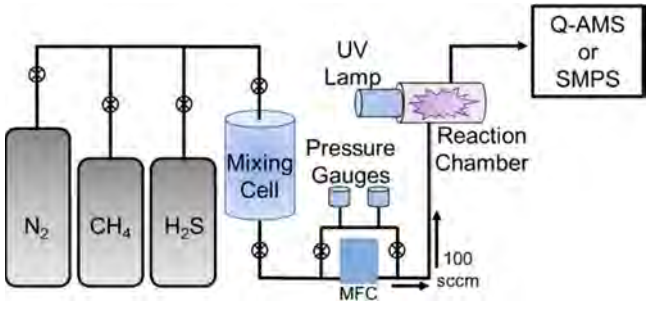

Figure 1. Schematic of the haze formation flow system. Flow from the reaction chamber continues to either a Q-AMS or SMPS with a dilution flow specific for the instrument requirements.

A mass flow controller (MFC, Millipore, FC-2901 V) set the precursor mixture flow from the mixing cell into the stainless-steel reaction chamber (volume 300 cm^3) at 100 standard cm^3 per minute (sccm). In the reaction chamber, a water-cooled deuterium lamp (Hamamatsu, L1825) irradiates the gases. The lamp has continuous emission over the range 115 to 400 nm and peak emission between 115 and 165 nm. Figure 2 shows the lamp flux and absorption cross sections of CH_4 and H_2S as a function of wavelength.

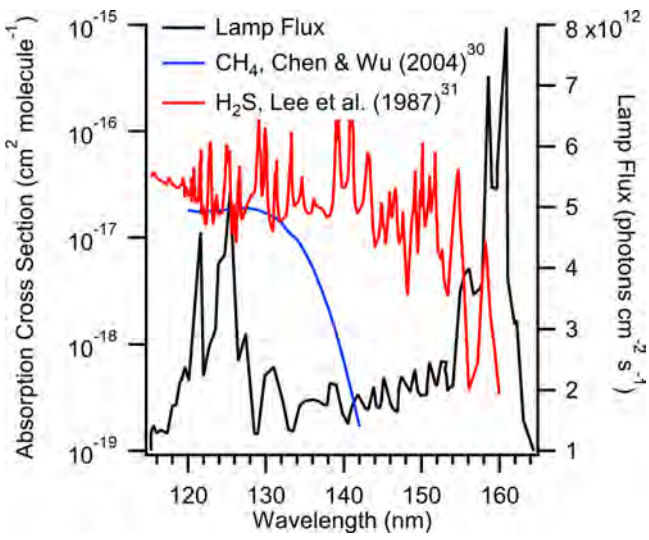

Figure 2. Absorption cross sections (cm^2 $molecule^{-1}$, left axis) for CH_4 (blue)[30] and H_2S (red)[31] and lamp flux (cm^{-2} s^{-1}, right axis) (black, provided by the manufacturer) as a function of wavelength in the range of the lamp's peak emission.

The lamp emission includes the Lyman-α line at 121.6 nm, which is the primary wavelength for CH_4 photolysis in planetary atmospheres in the solar system.[32] The primary pathways and products of CH_4 photodissociation at 121.6 nm are shown in reactions 1a and 1b, where Φ_{1a} and Φ_{1b} are the quantum yields of each pathway.[32]

$$CH_4 \xrightarrow{h\nu} H\cdot + \cdot CH_3, \quad \Phi_{1a} = 0.41 \tag{1a}$$

$$CH_4 \xrightarrow{h\nu} H_2 + CH_2, \quad \Phi_{1b} = 0.53 \tag{1b}$$

In the experiments presented here, the precursor mixtures are optically thick at wavelengths below ~145 nm due to the high methane concentration. H_2S, however, has a significant absorption cross section at wavelengths outside the range of CH_4 absorption. H_2S will photodissociate at 156.7 nm with the major pathway shown in reaction 2.[33,34] H_2S also photodissociates at 121.6 nm to produce H radicals and elemental sulfur, S.[34] However, as the reaction mixture is optically thick at 121.6 nm, this pathway is a negligible contribution.

https://dx.doi.org/10.1021/acsearthspacechem.0c00086
ACS Earth Space Chem. 2020, 4, 897−904

$$H_2S \xrightarrow{h\nu} H\cdot + HS\cdot(X^2\Pi), \quad h\nu = 156.7\ \text{nm} \qquad (2)$$

Products formed in the UV reaction chamber continuously flow into either a quadrupole aerosol mass spectrometer (Q-AMS) or scanning mobility particle sizer (SMPS) for measurements of aerosol composition or mobility size distribution, respectively. A nitrogen gas dilution of ∼20 sccm and ∼200 sccm is added for the AMS and SMPS, respectively, due to instrument flow requirements. Experiments were conducted under ambient pressures and temperatures, ∼630 Torr and ∼20 °C, respectively.

Quadrupole Aerosol Mass Spectrometry (Q-AMS). The Q-AMS, previously described in detail, provides quantitative measurements of the total aerosol mass loading, chemical composition, and aerodynamic size.[35−37] Briefly, an aerodynamic lens focuses aerosol particles into a beam through a vacuum chamber while trace gases are differentially pumped away. The particle beam is modulated by a chopper that can block the particle beam ("beam closed" position), allow the particle beam to pass through freely ("beam open" position), or "chops" the beam into packets at a user-defined rate (100−150 Hz) ("chopped" position). In the "chopped" position each opening of the chopper acts as the time-zero point before the beam passes through a vacuum time-of-flight region.[37] Aerosols are then flash vaporized at ∼600 °C into gas-phase molecules, ionized by electron ionization (EI) at 70 eV, and detected using quadrupole mass spectrometry (QMA 410, Balzers, Liechtenstein) with unit-mass resolution. The Q-AMS measurement mode was alternated between mass spectrum (MS) and particle time-of-flight (PTOF) modes for real-time measurements of aerosol mass loading/chemical composition and vacuum aerodynamic diameter (D_{va}) particle size distribution, respectively. In MS mode, the chopper alternates between "beam open" and "beam closed" positions every 5 s. In PTOF mode, the chopper is set to "chopped" position.[37] All mass spectra are reported as difference spectra between the beam open and beam closed modes and report only the aerosol-phase compositions. Major gas-phase species, predominately N_2 in this instance, are unable to be completely pumped away; this is referred to as a background gas or air beam. Background spectra of the air beam are acquired for each experiment before particles are produced and these background spectra are subtracted from the aerosol spectra collected, thus omitting any detected gas-phase interference. The aerosol mass loading of each spectra is quantitatively determined using the ion signals, sample flow rate, and ionization efficiency as described previously in detail in standard AMS analysis methods.[37]

Scanning Mobility Particle Sizer (SMPS). A SMPS is used to measure the number of particles as a function of their electrical mobility diameter (D_m) over a size range of 14.3 to 673 nm. The SMPS setup consists of a differential mobility analyzer (DMA, TSI, model 3081) connected to a condensation particle counter (CPC, TSI, model 3775). Polydisperse aerosol particles are charged by a ^{85}Kr charger before entering the DMA. In the DMA, aerosols are size selected based on their D_m against a drag force of air. The CPC counts the number of particles via light scattering at each D_m.

RESULTS AND DISCUSSION

Aerosol Mass Loading, Chemical Composition, and Organosulfur Formation. The AMS measurements provide insight into how the addition of H_2S alters the aerosol mass loading and composition. Figure 3A shows representative absolute mass spectra of aerosol produced using 0.1% CH_4 in N_2 with either 0, 1, or 5 ppmv H_2S included in the initial gas mixture. The absolute signal at nearly each m/z increased as the initial H_2S mixing ratio was increased. Furthermore, total aerosol mass loading increased appreciably as the initial H_2S mixing ratio was increased (Figure 4) with a mass enhancement factor of 2.8 measured at 5 ppmv H_2S. The mass enhancement factor was calculated as the ratio of mass loading for a given experiment to that of the 0 ppmv H_2S experiment. This result indicates that even ppmv amounts of H_2S, compared to percent amounts of CH_4, broadly enhanced the production of organic compounds without any additional carbon source in the precursor mixture.

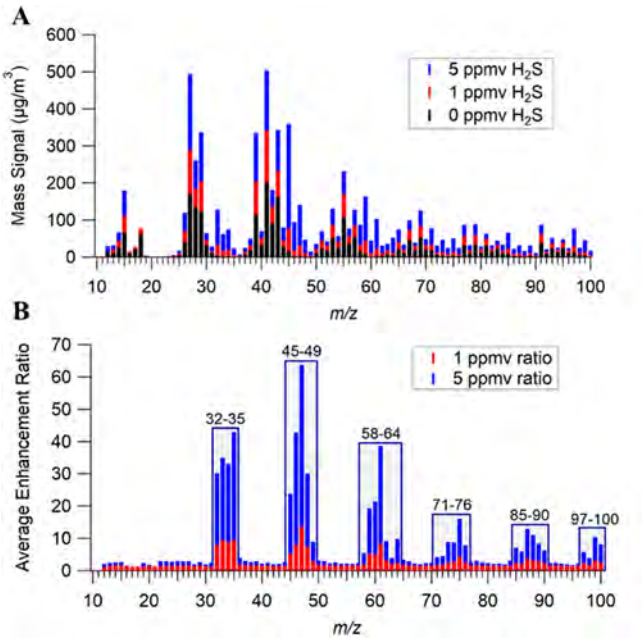

Figure 3. (A) Superimposed representative mass spectra of aerosol produced by gas mixtures consisting of 5 ppmv H_2S (blue), 1 ppmv H_2S (red), or 0 ppmv H_2S (black) with 0.1% CH_4 in N_2. (B) Superimposed ratios of the average absolute signals at each m/z (Average Enhancement Ratio) of experiments with 1 or 5 ppmv H_2S to experiments without H_2S in 0.1% CH_4 in N_2.

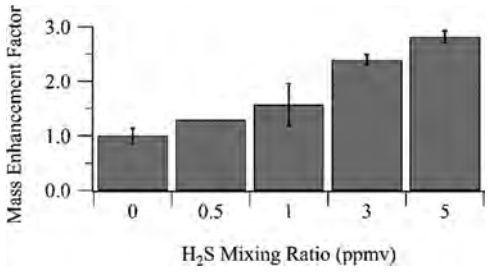

Figure 4. Total organic aerosol mass loading enhancements as a function of H_2S mixing ratio. Enhancements are calculated relative to the average 0 ppmv H_2S mass loading. Error bars signify 2 standard errors of the mean centered at the average mass loading. Only one experiment of 0.5 ppmv H_2S was conducted due to subsequent failure of the deuterium lamp.

In addition to increased aerosol mass, several compositional changes are observed in the mass spectra produced from

https://dx.doi.org/10.1021/acsearthspacechem.0c00086
ACS Earth Space Chem. 2020, 4, 897−904

mixtures that included trace H_2S. The compositional changes between the mass spectra are further illustrated in Figure 3B, which shows the ratio of the average absolute signals at each m/z for the 1 and 5 ppmv H_2S experiments to the average absolute signal at each m/z for experiments without H_2S. This ratio is referred to as the average enhancement ratio. Note that there is an enhancement at nearly each m/z. Particular mass ranges are clearly more enhanced than the rest, as highlighted in the figure, and illustrate the most significant changes in composition. These changes in composition are consistent with the formation of organosulfur compounds. Notably, there is an appearance of ions at m/z 32, 33, 34, and 35, interpreted as S^+, HS^+, H_2S^+, and H_3S^+, respectively, in the mass spectra of aerosol generated from the mixtures with H_2S (Figure 3A and Figure 3B). Note that the origins of m/z 32−35 are from the aerosol, not gas-phase H_2S, as discussed in Materials and Methods. These ions are characteristic EI fragments of organic thiols and sulfides and therefore provide evidence for organosulfur formation.[38] The relative intensities of m/z 32, 33, and 34 are higher than expected for EI spectra of organic thiols and sulfides. This is likely the result of thermally induced elimination of H_2S from thiols and sulfides during vaporization on the AMS heater.[39] Analogous thermal dehydration of alcohols is a well-known occurrence in AMS measurements.[40] The H_2S formed from thermal decomposition on the heater can be ionized resulting in high relative intensities for m/z 32, 33, and 34.

The Q-AMS used here is limited to unit mass resolution (UMR). Furthermore, the Q-AMS provides information on the bulk chemical composition but does not provide molecular level information, and the likelihood of isobaric ions increases at higher m/z. Because of these factors, the exact chemical formulas of individual mass-to-charge ratios cannot be explicitly determined. However, educated interpretations about the bulk compositions can be made by considering the likely products formed during the experiments based on known chemistry and common EI mass spectrum fragmentation patterns of compounds. Aerosol compositional changes were therefore interpreted in further detail using delta analysis.[38] Delta analysis is a mass spectra analysis method for organic molecules in which the ions are interpreted based on common fragmentation patterns. The ions are classified by delta (Δ) values, each a series of ions separated by 14 mass units (equivalent to a CH_2 unit), calculated by eq 3:

$$\Delta = m - 14n + 1 \tag{3}$$

where m is the m/z of the ion of interest and n is physically interpreted as the number of carbons of a standard alkene fragment and produces a Δ value between −7 and +6. The fraction of total signal of each Δ series allows for a bulk analysis of the aerosol composition.

The Δ series exhibiting the largest fractional increase as a function of H_2S mixing ratio (Figure 5A) were Δ = +4 (m/z 45, 59, 73, 87, and 101) followed by Δ = +6 (m/z 33, 47, 61, 75, 89, and 103), and Δ = +5 (m/z 32, 46, 60, 74, 88, 102, and 116). These were interpreted as fragments of unsaturated thiols/sulfides, alkyl thiols/sulfides, and cyclic sulfides,[38] respectively, thus providing further evidence for organosulfur formation. The ions of these Δ series are observed in the enhanced mass ranges highlighted in Figure 3B. Further, the ions of the enhanced mass ranges excluded from the delta analysis are also consistent with organosulfur EI fragments.[38,41]

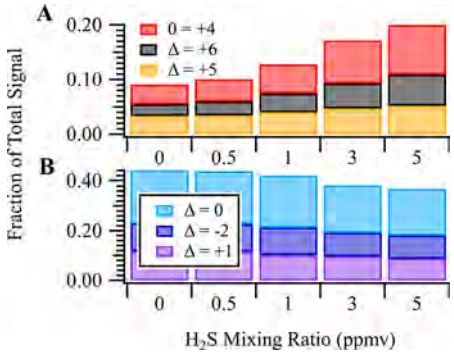

Figure 5. (A) Δ series that increased in fraction of total signal as a function of H_2S mixing ratio, which correspond to unsaturated thiols and sulfides (Δ = +4), alkyl thiols and sulfides (Δ = +6), and cyclic sulfides (Δ = +5). (B) Δ series that decreased as a function of H_2S mixing ratio, which broadly correspond to unsaturated hydrocarbons: alkenes and cycloalkanes (Δ = 0), dienes, alkynes, and cycloalkenes (Δ = −2), and terminal alkenes or alkenyl/cyclic amines ($C_nH_{2n}N$) (Δ = +1).

The Δ series exhibiting the largest fractional decrease as a function of H_2S mixing ratio (Figure 5B) were Δ = 0 (m/z 27, 41, 55, 69, and 83), followed by Δ = −2 (m/z 53, 67, 81, 95, 109, and 123), and Δ = +1 (m/z 14, 28, 42, 56, and 70). These Δ series correspond to what can broadly be categorized as unsaturated hydrocarbons.[38] The Δ = 0 series is indicative of alkenes and cycloalkanes, Δ = −2 of dienes, alkynes, and cycloalkenes, and Δ = +1 of terminal alkenes or alkenyl/cyclic amines ($C_nH_{2n}N$).[38] Note that organic nitrogen compounds have previously been observed in the aerosol products of similar haze experiments, even though N_2 does not photodissociate at the wavelengths used in this experiment. Possible mechanisms for nitrogen incorporation have previously been discussed in detail; however, no conclusive mechanism has been identified (see Trainer et al. (2012);[25] Sebree et al.;[42] Berry et al.;[43] Berry et al.,[23] and references therein). These fractional decreases could imply that unsaturated hydrocarbons contribute less to the overall composition of the organic aerosol due to reactions leading to organosulfur formation.

The compositional analyses of the mass spectra are inconsistent with the formation of inorganic sulfur aerosol. The ion series for elemental sulfur (S_8) aerosol (m/z 64, 96, 128, 160, and 192)[41] and H_2SO_4 aerosol (m/z 48, 64, 80, 81, and 98)[41] both show negligible enhancement. While m/z 48 and 64 are observed to increase upon the addition of H_2S, the ratio between the two ions is inconsistent with the measured ion ratio of sulfate aerosol, expected to be ∼1. We therefore attribute m/z 48 to SCH_4^+. Furthermore, the m/z 80 and 81 signals do not show significant enhancement, implying that H_2SO_4 aerosol is unlikely. The absence of an increase in m/z 96 and the relatively low m/z 64 signal compared to the m/z 32 signal further suggests that sulfur chain formation is unlikely.

Aerosol Particle Size and Effective Density. Combined measurements of the vacuum aerodynamic diameter (D_{va}, measured by the PTOF mode of the AMS) and the volume-weighted mode mobility diameter (D_m, measured by the SMPS) of the aerosol particles allow for a calculation of the particle effective density (ρ_{eff}) via eq 4:

$$\rho_{eff} = \rho_\circ \frac{D_{va}}{D_m} \tag{4}$$

https://dx.doi.org/10.1021/acsearthspacechem.0c00086
ACS Earth Space Chem. 2020, 4, 897−904

where ρ_o is unit density (1 g cm^{-3}).[44]

D_{va} increased as the initial mixing ratio of H_2S increased (Figure 6). In contrast, D_m remained relatively constant with the addition of H_2S to the precursor mixture (Figure 6.).

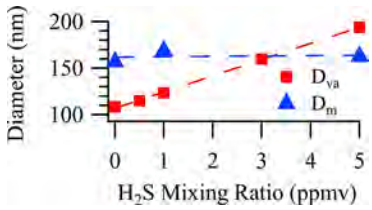

Figure 6. Volume-weighted mode mobility diameter (D_m, nm) (blue) and vacuum aerodynamic diameter (D_{va}, nm) (red) as a function of initial H_2S mixing ratio.

This observation that D_m remains relatively constant while D_{va} increases as a function of initial H_2S mixing ratio implies that the particle effective density increased as the initial H_2S mixing ratio increased (Table 1).

Table 1. Particle Effective Density (ρ_{eff}, g/cm^3) for Each Experiment

gas mixture in N_2	ρ_{eff} (g/cm^3)
0.1% CH_4[a]	0.65 ± 0.11[a]
0.1% CH_4	0.69
1 ppmv H_2S, 0.1% CH_4	0.73 ± 0.04
5 ppmv H_2S, 0.1% CH_4	1.20 ± 0.06

[a]From Horst and Tolbert.[24] Errors represent two standard errors of the mean.

Although proportional to material density, effective density is influenced by the shape and porosity of the particles.[44] Previous work has found that the particles formed by UV irradiation of 0.1% CH_4 in N_2 mixtures are spherical.[26] Since we do not expect the addition of H_2S to significantly alter the particle shape or porosity, the increase in effective density is likely due to an increase in material density. Similar increases in particle effective density have been reported when oxygen has been added to the precursor mixture.[20]

The formation of organic thiols and sulfides and the depletion of unsaturated hydrocarbons is consistent with an observed increase in particle effective density, which is proportional to the material density. This is because organic thiols and sulfides have a greater density than corresponding hydrocarbons of similar molecular weights (i.e., the density of 1-hexene[45] is 0.67 g/cm^3 while the density of butanethiol[46] is 0.83 g/cm^3 and that of diethyl sulfide[47] is 0.84 g/cm^3).

Possible Mechanism of Organosulfur Formation. On the basis of the mass spectral evidence presented above, we attribute the increase in organic haze mass to the formation of organosulfur compounds, such as thiols and sulfides. A hypothesized organosulfur production mechanism is shown in Figure 7. The mechanism begins with CH_4 photodissociation. Subsequent reactions form alkene or alkyne products (step 1). The HS radicals formed from H_2S photodissociation (step 2) react with the alkene or alkyne products to form substituted alkyl radicals (step 3). The initial substituted alkyl radicals could then form molecular products (i.e., thiols) by abstracting a hydrogen from another species (step 4) or through radical−radical recombination (not shown). Alternatively, the substituted alkyl radicals can react further with alkenes or alkynes resulting in carbon chain growth (step 5). As small thiols are known to photolyze at wavelengths within the lamp range and at wavelengths beyond the absorption of CH_4, thiol photolysis could form thiyl radicals (step 6).[48,49] Once formed, thiyl radicals can add to the pi bonds of alkenes or alkynes resulting in a sulfide bond (step 7) and a substituted alkyl radical.[48,49]

This sulfide alkyl radical can then form molecular products (i.e., sulfides) by abstracting a hydrogen from another species (step 8) or through radical−radical recombination (not shown). Alternatively, the sulfide alkyl radical can react with alkenes or alkynes resulting in further carbon chain growth (step 9). Products from steps 5 and 9 may undergo hydrogen abstraction, radical−radical recombination, or further chain growth. Efficient chain growth would favor molecular partitioning into the particle phase, which could explain the

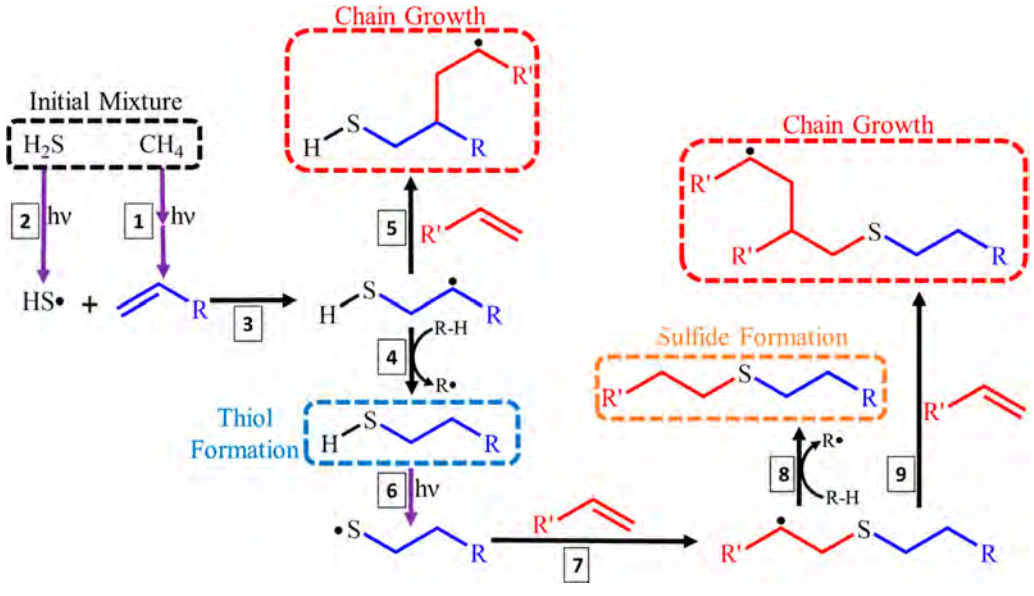

Figure 7. Proposed reaction mechanism for organosulfur formation in the current experiments.

https://dx.doi.org/10.1021/acsearthspacechem.0c00086
ACS Earth Space Chem. 2020, 4, 897−904

overall observed increase in organic aerosol signal. Further, as shown in Figure 7, H_2S photolysis initiates radical chemistry that could lead to radical propagation and chain growth (steps 3, 5, 7, and 9), and is thus a possible explanation for the overall enhancement of organic compounds. Arney et al. (2018)[15] proposed that the photochemistry of organosulfur gases could enhance organic haze formation by acting as an additional hydrocarbon radical source.[15] However, we have shown that the photochemistry of H_2S, a noncarbon gas, also enhances organic aerosol formation without any additional carbon source.

The chemistry of HS and thiyl radicals reacting with alkenes and alkynes and the production of organosulfur is currently absent from models and considerations of planetary haze formation chemistry. However, analogous chemistry has been proposed in other studies. For example, Tsukada et al.[50] observed that gas-phase UV photochemical reactions of H_2S and acetylene yielded gas-phase thiophene.[50] Arthur et al.[51] also found that gas-phase photochemical reactions of H_2S and ethylene produced thiols and sulfides.[51] The mechanisms proposed in Tsukada et al.[50] and Arthur et al.[51] both involved HS radical additions to alkene/alkyne pi bonds, consistent with the mechanism proposed in this work. Analogous fast gas-phase reactions of hydroxyl radicals (OH) with alkenes and alkynes have been well-established, where OH adds to pi bonds.[52] Further, UV-initiated thiol-alkene chemistry is known to be highly efficient in solution, including effective radical propagation and chain growth, and is the basis of high-yield radical polymerization reactions in organic and materials synthesis methods.[53,54] Applied to the context of our studies, this thiol-alkene photochemistry can have a potential impact on the understanding organic haze formation processes in planetary atmospheres.

Impact of Sulfur on Planetary Organic Haze Chemistry. The observation of significant organosulfur formation stands in contrast to previous assumptions that sulfur gases primarily form S_8 or H_2SO_4 aerosols and instead suggests direct interactions between carbon and sulfur chemistry. Organosulfur formation has also been previously observed by DeWitt et al.[16] in similar experiments to the present study, although $SO_2/CH_4/N_2$ mixtures were studied.[16] The results of DeWitt et al.[16] differ from those presented here in that they observed the formation of inorganic sulfur aerosol, H_2SO_4 aerosol, in addition to organosulfur aerosol. In the present study using H_2S, the sulfur was incorporated into the aerosol exclusively in the form of reduced organosulfur compounds, with no compelling evidence for the formation of S_8 or H_2SO_4.

Further, a recent study by He et al.[55] also observed organosulfur formation and increased aerosol production in experiments using $CO_2/CO/N_2/H_2/H_2O$/He mixtures (without added methane) with higher mixing ratios of H_2S (1.6%) and lower mixing ratios of N_2 (11%) than investigated here.[55] The experiments of He et al.[55] were also conducted at a higher temperature (800 K).[55] However, the results of He et al.[55] support the idea that organosulfur formation may be a common occurrence in a range of planetary atmospheres.[55]

The combination of our results and those of DeWitt et al.[16] and He et al.[55] show that in the presence of either H_2S or SO_2, organic haze chemistry can produce significant amounts of organosulfur.[16,55] Given these results, organosulfur aerosol may be common in organic hazes formed in the presence of inorganic sulfur gases. The formation of organosulfur aerosol provides a third pathway (in addition to S_8 and H_2SO_4) for sulfur to exit the atmosphere and thus may be of importance when considering the interpretation of the S-MIF geochemical record. In order to further investigate the potential impact of coupled sulfur-haze chemistry on the S-MIF, further experiments using precursor mixtures relevant to the Archean atmosphere are required. Our results suggest that $CH_4/CO_2/H_2S/SO_2/N_2$ mixtures should be investigated to better understand the interplay of the Archean Earth atmospheric sulfur cycle and organic haze chemistry.

Beyond the Archean Earth, organic hazes are thought to be important for the interpretation and characterization of exoplanetary atmospheres and their climates.[13,56] Depending on aerosol particle composition, size, and optical properties, a planetary organic haze can affect a planet's radiative forcing, thus influencing climate and habitability. We found that trace amounts of H_2S, a noncarbon gas, opens new reaction pathways that enhance organic aerosol formation and increases the effective density of the haze aerosol. Enhancement of organic aerosol formation could imply changes to the thickness and optical properties of an organic haze. Haze chemistry also leads to the formation of complex organic molecules, making organic haze of potential importance to the formation of prebiotic molecules. Since organosulfur is essential for biological molecules, the formation of organosulfur in sulfur-haze chemistry could further the prebiotic relevance of organic hazes.

CONCLUSIONS

The results of this work show that under the photochemical conditions considered here, inclusion of trace amounts of H_2S dramatically increases organic aerosol mass loading in the absence of an additional carbon source. Significant organosulfur formation was observed and is the only form of sulfur aerosol detected. Organosulfur formation is also the likely cause for the observed increase in particle effective density. When taken in combination with the results of DeWitt et al.[16] and He et al.,[55] these results indicate that organic haze composition is directly influenced by the photochemistry of inorganic sulfur gases. Although organosulfur is observed in modern Earth aerosol, the reactions responsible for organosulfur formation are typically missing from most models of other planetary atmospheres. In the case of the Archean atmosphere, the effects of H_2S on organic haze chemistry observed here could influence the interpretation of the S-MIF. It is clear that more studies are required to further investigate the effects of sulfur gases on haze chemistry in different atmospheric compositions, especially Archean-like atmospheric analogs.

AUTHOR INFORMATION

Corresponding Author

Eleanor C. Browne − *Department of Chemistry and Cooperative Institute for Research in Environmental Sciences, University of Colorado, Boulder, Colorado 80309, United States;* orcid.org/0000-0002-8076-9455; Phone: 303-735-7685; Email: eleanor.browne@colorado.edu

Authors

Nathan W. Reed − *Department of Chemistry and Cooperative Institute for Research in Environmental Sciences, University of Colorado, Boulder, Colorado 80309, United States;* orcid.org/0000-0002-0401-5993

https://dx.doi.org/10.1021/acsearthspacechem.0c00086
ACS Earth Space Chem. 2020, 4, 897−904

Margaret A. Tolbert − *Department of Chemistry and Cooperative Institute for Research in Environmental Sciences, University of Colorado, Boulder, Colorado 80309, United States;* orcid.org/0000-0001-5730-6412

Complete contact information is available at: https://pubs.acs.org/10.1021/acsearthspacechem.0c00086

Notes

The authors declare no competing financial interest.

■ ACKNOWLEDGMENTS

This work was supported by NASA grant 80NSSC20K0232.

■ ABBREVIATIONS

S-MIF, mass-independent fraction of sulfur isotopes; UV, ultraviolet; AMS, aerosol mass spectrometry; Q-AMS, quadrupole aerosol mass spectrometry; SMPS, scanning mobility particle sizer; MFC, mass flow controller; sccm, standard cubic centimeters per second; MS, mass spectra; PTOF, particle time-of-flight; D_{va}, vacuum aerodynamic diameter; D_m, volume-weighted electrical mobility diameter; DMA, differential mobility analyzer; CPC, condensation particle counter; EI, electron ionization; ρ, particle effective density.

■ REFERENCES

(1) Atreya, S. K.; Mahaffy, P. R.; Niemann, H. B.; Wong, M. H.; Owen, T. C. Composition and Origin of the Atmosphere of Jupiter - An Update, and Implications for the Extrasolar Giant Planets. *Planet. Space Sci.* **2003**, *51* (2), 105−112.

(2) Hu, R.; Seager, S.; Bains, W. Photochemistry in Terrestrial Exoplanet Atmospheres. II. H_2S and SO_2 Photochemistry in Anoxic Atmospheres. *Astrophys. J.* **2013**, *769* (1), 1−55.

(3) Gao, P.; Marley, M. S.; Zahnle, K.; Robinson, T. D.; Lewis, N. K. Sulfur Hazes in Giant Exoplanet Atmospheres: Impacts on Reflected Light Spectra. *Astron. J.* **2017**, *153* (3), 139.

(4) Lellouch, E. Io's Atmosphere and Surface-Atmosphere Interactions. *Space Sci. Rev.* **2005**, *116* (1−2), 211−224.

(5) Marcq, E.; Mills, F. P.; Parkinson, C. D.; Vandaele, A. C. Composition and Chemistry of the Neutral Atmosphere of Venus. *Space Sci. Rev.* **2018**, *214* (1), 1−55.

(6) Farquhar, J.; Wing, B. A. Multiple Sulfur Isotopes and the Evolution of the Atmosphere. *Earth Planet. Sci. Lett.* **2003**, *213* (1−2), 1−13.

(7) Kasting, J. F.; Zahnle, K. J.; Pinto, J. P.; Young, A. T. Sulfur, Ultraviolet Radiation, and the Early Evolution of Life. *Origins Life Evol. Biospheres* **1989**, *19*, 95−108.

(8) Pavlov, A. A.; Kasting, J. F. Mass-Independent Fractionation of Sulfur Isotopes in Archean Sediments: Strong Evidence for an Anoxic Archean Atmosphere. *Astrobiology* **2002**, *2* (1), 27−41.

(9) Tolocka, M. P.; Turpin, B. Contribution of Organosulfur Compounds to Organic Aerosol Mass. *Environ. Sci. Technol.* **2012**, *46* (15), 7978−7983.

(10) Zerkle, A. L.; Claire, M. W.; Domagal-Goldman, S. D.; Farquhar, J.; Poulton, S. W. A Bistable Organic-Rich Atmosphere on the Neoarchaean Earth. *Nat. Geosci.* **2012**, *5* (5), 359−363.

(11) Izon, G.; Zerkle, A. L.; Zhelezinskaia, I.; Farquhar, J.; Newton, R. J.; Poulton, S. W.; Eigenbrode, J. L.; Claire, M. W. Multiple Oscillations in Neoarchaean Atmospheric Chemistry. *Earth Planet. Sci. Lett.* **2015**, *431*, 264−273.

(12) Domagal-Goldman, S. D.; Kasting, J. F.; Johnston, D. T.; Farquhar, J. Organic Haze, Glaciations and Multiple Sulfur Isotopes in the Mid-Archean Era. *Earth Planet. Sci. Lett.* **2008**, *269* (1−2), 29−40.

(13) Arney, G.; Domagal-Goldman, S. D.; Meadows, V. S.; Wolf, E. T.; Schwieterman, E.; Charnay, B.; Claire, M.; Hébrard, E.; Trainer, M. G. The Pale Orange Dot: The Spectrum and Habitability of Hazy Archean Earth. *Astrobiology* **2016**, *16* (11), 873−899.

(14) Liu, P.; Harman, C. E.; Kasting, J. F.; Hu, Y.; Wang, J. Can Organic Haze and O_2 Plumes Explain Patterns of Sulfur Mass-Independent Fractionation during the Archean? *Earth Planet. Sci. Lett.* **2019**, *526*, 115767.

(15) Arney, G.; Domagal-Goldman, S. D.; Meadows, V. S. Organic Haze as a Biosignature in Anoxic Earth-like Atmospheres. *Astrobiology* **2018**, *18* (3), 311−329.

(16) Dewitt, H. L.; Hasenkopf, C. A.; Trainer, M. G.; Farmer, D. K.; Jimenez, J. L.; McKay, C. P.; Toon, O. B.; Tolbert, M. A. The Formation of Sulfate and Elemental Sulfur Aerosols under Varying Laboratory Conditions: Implications for Early Earth. *Astrobiology* **2010**, *10* (8), 773−781.

(17) Aiuppa, A.; Inguaggiato, S.; McGonigle, A. J. S.; O'Dwyer, M.; Oppenheimer, C.; Padgett, M. J.; Rouwet, D.; Valenza, M. H2S Fluxes from Mt. Etna, Stromboli, and Vulcano (Italy) and Implications for the Sulfur Budget at Volcanoes. *Geochim. Cosmochim. Acta* **2005**, *69* (7), 1861−1871.

(18) Kump, L. R.; Barley, M. E. Increased Subaerial Volcanism and the Rise of Atmospheric Oxygen 2.5 Billion Years Ago. *Nature* **2007**, *448* (7157), 1033−1036.

(19) Kump, L. R.; Pavlov, A.; Arthur, M. A. Massive Release of Hydrogen Sulfide to the Surface Ocean and Atmosphere during Intervals of Oceanic Anoxia. *Geology* **2005**, *33* (5), 397−400.

(20) Ugelow, M. S.; Haan, D. O. De; Hörst, S. M.; Tolbert, M. A. The Effect of Oxygen on Organic Haze Properties. *Astrophys. J., Lett.* **2018**, *859* (1), L2.

(21) Hörst, S. M.; He, C.; Ugelow, M. S.; Jellinek, A. M.; Pierrehumbert, R. T.; Tolbert, M. A. Exploring the Atmosphere of Neoproterozoic Earth: The Effect of O_2 on Haze Formation and Composition. *Astrophys. J.* **2018**, *858* (2), 119.

(22) Shen, Y.; Buick, R. The Antiquity of Microbial Sulfate Reduction. *Earth-Sci. Rev.* **2004**, *64* (3−4), 243−272.

(23) Berry, J. L.; Ugelow, M. S.; Tolbert, M. A.; Browne, E. C. Chemical Composition of Gas-Phase Positive Ions during Laboratory Simulations of Titan's Haze Formation. *ACS Earth Sp. Chem.* **2019**, *3* (2), 202−211.

(24) Hörst, S. M.; Tolbert, M. A. In Situ Measurements of the Size and Density of Titan Aerosol Analogs. *Astrophys. J., Lett.* **2013**, *770* (1), 1−6.

(25) Trainer, M. G.; Jimenez, J. L.; Yung, Y. L.; Toon, O. B.; Tolbert, M. A. Nitrogen Incorporation in CH_4-N_2 Photochemical Aerosol Produced by Far Ultraviolet Irradiation. *Astrobiology* **2012**, *12* (4), 315−326.

(26) Trainer, M. G.; Pavlov, A. A.; DeWitt, H. L.; Jimenez, J. L.; McKay, C. P.; Toon, O. B.; Tolbert, M. A. Organic Haze on Titan and the Early Earth. *Proc. Natl. Acad. Sci. U. S. A.* **2006**, *103* (48), 18035−18042.

(27) Izon, G.; Zerkle, A. L.; Williford, K. H.; Farquhar, J.; Poulton, S. W.; Claire, M. W. Biological Regulation of Atmospheric Chemistry En Route to Planetary Oxygenation. *Proc. Natl. Acad. Sci. U. S. A.* **2017**, *114* (13), E2571−E2579.

(28) Holland, H. D. Volcanic Gases, Black Smokers, and the Great Oxidation Event. *Geochim. Cosmochim. Acta* **2002**, *66* (21), 3811−3826.

(29) Archer, C.; Vance, D. Coupled Fe and S Isotope Evidence for Archean Microbial Fe(III) and Sulfate Reduction. *Geology* **2006**, *34* (3), 153−156.

(30) Chen, F. Z.; Wu, C. Y. R. Temperature-Dependent Photoabsorption Cross Sections in the VUV-UV Region. I. Methane and Ethane. *J. Quant. Spectrosc. Radiat. Transfer* **2004**, *85*, 195−209.

(31) Lee, L. C.; Wang, X.; Suto, M. Quantitative Photoabsorption and Fluorescence Spectroscopy of H_2S and D_2S at 49−240 Nm. *J. Chem. Phys.* **1987**, *86* (8), 4353−4361.

(32) Smith, N. S.; Raulin, F. Modeling of Methane Photolysis in the Reducing Atmospheres of the Outer Solar System. *J. Geophys. Res. E Planets* **1999**, *104* (E1), 1873−1876.

(33) Liu, X.; Hwang, D. W.; Yang, X. F.; Harich, S.; Lin, J. J.; Yang, X. Photodissociation of Hydrogen Sulfide at 157.6 Nm: Observation

of SH Bimodal Rotational Distribution. *J. Chem. Phys.* **1999**, *111* (9), 3940−3945.
(34) Chakraborty, S.; Jackson, T. L.; Ahmed, M.; Thiemens, M. H. Sulfur Isotopic Fractionation in Vacuum UV Photodissociation of Hydrogen Sulfide and Its Potential Relevance to Meteorite Analysis. *Proc. Natl. Acad. Sci. U. S. A.* **2013**, *110* (44), 17650−17655.
(35) Jimenez, J. L.; Jayne, J. T.; Shi, Q.; Kolb, C. E.; Worsnop, D. R.; Yourshaw, I.; Seinfeld, J. H.; Flagan, R. C.; Zhang, X.; Smith, K. A.; Morris, J. W.; Davidovits, P. Ambient Aerosol Sampling Using the Aerodyne Aerosol Mass Spectrometer. *J. Geophys. Res.* **2003**, *108*, 1−13.
(36) Jayne, J. T.; Leard, D. C.; Zhang, X.; Davidovits, P.; Smith, K. A.; Kolb, C. E.; Worsnop, D. R. Development of an Aerosol Mass Spectrometer for Size and Composition Analysis of Submicron Particles. *Aerosol Sci. Technol.* **2000**, *33*, 49−70.
(37) Allan, J. D.; Jimenez, J. L.; Williams, P. I.; Alfarra, M. R.; Jayne, J. T.; Coe, H.; Worsnop, D. R. Quantitative Sampling Using an Aerodyne Aerosol Mass Spectrometer 1. Techniques of Data Interpretation and Error Analysis. *J. Geophys. Res. D Atmos.* **2003**, *108*, 1−10.
(38) McLafferty, F. W.; Turecek, F. *Interpretation of Mass Spectra*, 4th ed.; University Science Books: Mill Valley, CA, 1993.
(39) Moldoveanu, S. C. *Tech. Instrum. Anal. Chem.* **2010**, *28*, 79.
(40) Canagaratna, M. R.; Jimenez, J. L.; Kroll, J. H.; Chen, Q.; Kessler, S. H.; Massoli, P.; Hildebrandt Ruiz, L.; Fortner, E.; Williams, L. R.; Wilson, K. R.; Surratt, J. D.; Donahue, N. M.; Jayne, J. T.; Worsnop, D. R. Elemental Ratio Measurements of Organic Compounds Using Aerosol Mass Spectrometry: Characterization, Improved Calibration, and Implications. *Atmos. Chem. Phys.* **2015**, *15* (1), 253−272.
(41) NIST Mass Spectrometry Data Center; Wallace, W. E. Mass Spectra in *NIST Chemistry WebBook, NIST Standard Reference Database Number 69*; Linstrom, P.J., Mallard, W.G., Eds.; National Institute of Standards and Technology: Gaithersburg MD, 20899. DOI: 10.18434/T4D303, (retrieved March 31, 2020).
(42) Sebree, J. A.; Roach, M. C.; Shipley, E. R.; He, C.; Hörst, S. M. Detection of Prebiotic Molecules in Plasma and Photochemical Aerosol Analogs Using GC/MS/MS Techniques. *Astrophys. J.* **2018**, *865* (2), 133.
(43) Berry, J. L.; Ugelow, M. S.; Tolbert, M. A.; Browne, E. C. The Influence of Gas-Phase Chemistry on Organic Haze Formation. *Astrophys. J., Lett.* **2019**, *885* (1), L6.
(44) DeCarlo, P. F.; Slowik, J. G.; Worsnop, D. R.; Davidovits, P.; Jimenez, J. L. Particle Morphology and Density Characterization by Combined Mobility and Aerodynamic Diameter Measurements. Part 1: Theory. *Aerosol Sci. Technol.* **2004**, *38* (12), 1185−1205.
(45) National Center for Biotechnology Information. PubChem Database. *1-Hexene, CID = 11597*, https://pubchem.ncbi.nlm.nih.gov/compound/1-Hexene (accessed on Mar. 31, 2020).
(46) National Center for Biotechnology Information. PubChem Database. *2-Butanethiol, CID = 10560*, https://pubchem.ncbi.nlm.nih.gov/compound/2-Butanethiol (accessed on Mar. 31, 2020).
(47) National Center for Biotechnology Information. PubChem Database. *Diethyl sulfide, CID = 9609*, https://pubchem.ncbi.nlm.nih.gov/compound/Diethyl-sulfide (accessed on Mar. 31, 2020).
(48) Caspari, G.; Granzow, A. The Flash Photolysis of Mercaptans in Aqueous Solution. *J. Phys. Chem.* **1970**, *74* (4), 836−839.
(49) Skerrett, N. P.; Thompson, N. W. The Photolysis of Mercaptans. *Trans. Faraday Soc.* **1941**, *37*, 81−82.
(50) Tsukada, M.; Oka, T.; Shida, S. Photochemical and Radiation-Induced Reactions of Acetylene and Hydrogen Sulfide Mixture. Synthesis of Thiophene. *Chem. Lett.* **1972**, *1*, 437−440.
(51) Arthur, N. L.; Bell, T. N. 950. Photchemical Addition of Hydrogen Sulphide to C2 Olefins. *J. Chem. Soc.* **1962**, 4866−4870.
(52) Atkinson, R. Kinetics and Mechanisms of the Gas-Phase Reactions of the Hydroxyl Radical with Organic Compounds under Atmospheric Conditions. *Chem. Rev.* **1986**, *86* (1), 69−201.
(53) Northrop, B. H.; Coffey, R. N. Thiol-Ene Click Chemistry: Computational and Kinetic Analysis of the Influence of Alkene Functionality. *J. Am. Chem. Soc.* **2012**, *134* (33), 13804−13817.
(54) Tasdelen, M. A.; Yagci, Y. Light-Induced Click Reactions. *Angew. Chem., Int. Ed.* **2013**, *52* (23), 5930−5938.
(55) He, C.; Hörst, S. M.; Lewis, N. K.; Yu, X.; Moses, J. I.; McGuiggan, P.; Marley, M. S.; Kempton, E. M. R.; Moran, S. E.; Morley, C. V.; Vuitton, V. Sulfur-Driven Haze Formation in Warm CO_2-Rich Exoplanet Atmospheres. *Nat. Astron.* **2020**, 1−8.
(56) Marley, M. S.; Ackerman, A. S.; Cuzzi, J. N.; Kitzmann, D. Clouds and Hazes in Exoplanet Atmospheres. *Comp. Climatol. Terr. Planets* **2013**, 1−51.